Materials Chemistry and Physics 258 (2021) 123810

Contents lists available at ScienceDirect

Materials Chemistry and Physics

journal homepage: www.elsevier.com/locate/matchemphys

A silica-coated metal-organic framework/graphite-carbon nitride hybrid for improved fire safety of epoxy resins

Wenzong Xu [a,*], Hongyi Yan [a], Guisong Wang [b], Zhongqiong Qin [a], Liangjie Fan [a], Yuxiong Yang [a]

[a] School of Materials Science and Chemical Engineering, Anhui Jianzhu University, 292 Ziyun Road, Hefei, Anhui, 230601, PR China
[b] Lai'an Hengtong Rubber & Plastic Products Co., Ltd, 241 Yongyang East Road, Chuzhou, Anhui, 239200, PR China

HIGHLIGHTS

- A novel modified carbon nitride (ZIF-67/g-C3N4@SiO2) nano-hybrid containing Co and Si was first synthesized.
- ZIF-67/g-C3N4@SiO2 nano-hybrid can significantly reduce the heat, smoke and CO production of EP.
- A possible mechanism for inhibiting the ignition hazard of EP nanocomposites was proposed.

GRAPHICAL ABSTRACT

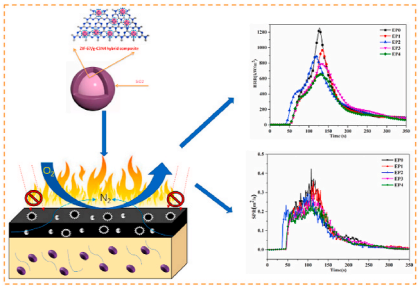

ARTICLE INFO

Keywords:
Epoxy resin
Hybrid material
Flame retardance
Smoke depressing

ABSTRACT

To reduce the fire hazard of epoxy resin (EP), ZIF-67/g-C_3N_4@SiO_2 (ZCS) hybrid material was prepared by electrostatic interaction and sol-gel method. The structure and morphology of ZCS were investigated by flourier transform infrared spectrometer, X-ray diffraction and scanning electron microscope. It was found that the latent fire hazard of EP was reduced via the addition of ZCS hybrid material. The EP composite with 3 wt% of ZCS had better fire safety than EP. Cone results showed that the heat and smoke emissions of EP composites were reduced to varying degrees, and specifically their peak heat release rate, total heat release rate, peak smoke production rate and total smoke production were reduced by 46.8%, 21.7%, 45.2% and 19.3%, respectively. In addition, the possible flame retardance and smoke depression mechanism of ZCS hybrid material is also discussed in this article.

1. Introduction

Zeolite imidazole frameworks (ZIFs) are a new kind of porous material synthesized by transition metal atoms (such as Zn, Co, etc.) and imidazole or imidazole derivative ligands in methanol solution [1–3]. Because of its excellent pore structure, large surface area, chemical and thermal stability, it is widely used in adsorption, separation, drug delivery and flame retardant filler or other field [4,5]. ZIF-67, a typical representative of ZIFs, is synthesized from Co^{2+} and 2-methylimidazole [6]. It has been shown that ZIF-67 is a material containing transition metal element Co and a large amount of N. There have been studies using metal oxides as polymer flame retardant synergists and smoke depressants [7,8]. Xu et al. successfully prepared ZIF-67/RGO-B nanometer materials and explored their effect on reducing the hidden fire risk

* Corresponding author.
E-mail address: wenzongxu@ahjzu.edu.cn (W. Xu).

https://doi.org/10.1016/j.matchemphys.2020.123810
Received 23 July 2020; Received in revised form 30 August 2020; Accepted 2 September 2020
Available online 29 September 2020
0254-0584/

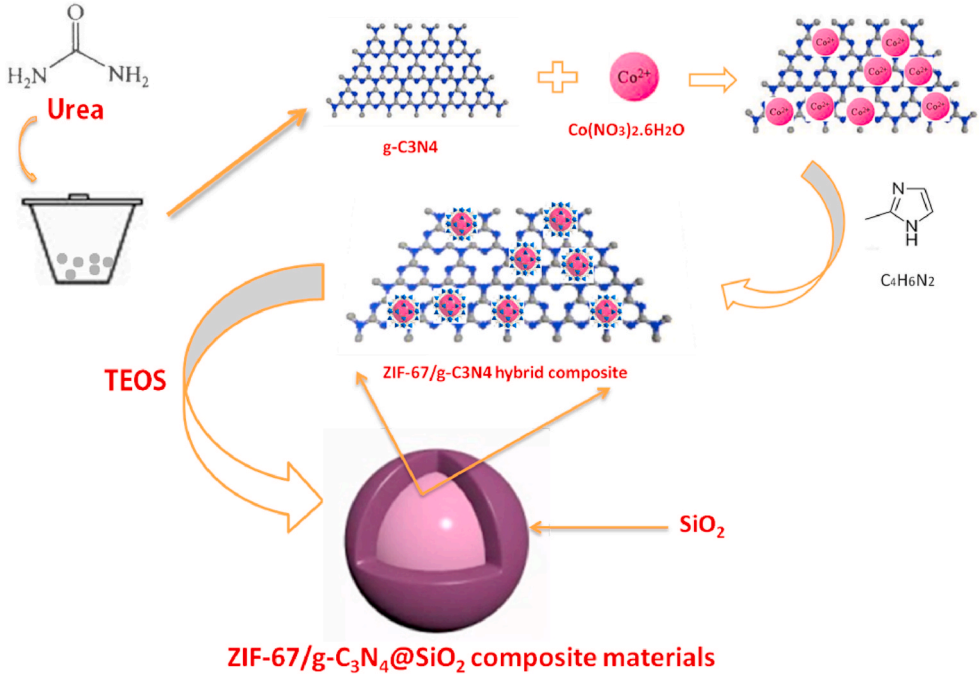

Scheme 1. Synthetic route of ZIF-67/g-C_3N_4@SiO_2 composite materials.

of EP. Their results indicated that the heat production rate and smoke emission amount of a composite decreased significantly with 2 wt% of ZIF-67/RGO-B [9].

Recently, montmorillonite [10], graphite carbon nitride (g-C_3N_4), grapheme, and other two-dimensional (2D) nanomaterials have attracted widespread attention in the field of flame retardant polymers. Among them, g-C_3N_4 composed of carbon and nitrogen elements, and its raw material is easy to obtain usually from high temperature polymerization of urea or melamine [11,12]. Owing to its unique electronic structure, high catalytic activity, good chemical and thermal stability, g-C_3N_4 has been used in catalysis, energy, hydrolysis to produce hydrogen and oxygen, pollutant degradation and other fields [13–16]. In recent years, g-C_3N_4 has attracted attention in the area of flame-retardant polymer composites. Shi et al. synthesized $CuCo_2O_4$/g-C_3N_4 nanohybrids, which reduced the dangerous properties of thermoplastic polyurethane (TPU). With 2 wt% $CuCo_2O_4$/g-C_3N_4 nanohybrids, their results showed that the THR and pHRR of TPU were reduced by 31.3% and 37% [17]. Zhu et al. used g-C_3N_4 and aluminum diethylphosphite to prepare the hybrid material CDAHPI to improve the flame retardancy of polystyrene (PS). They discovered that the introduction of 4 wt% of CDAHPI was able to reduce the pHRR and THR of PS compound material by 43% and 41%, respectively [18].

Epoxy resin (EP), with excellent chemical and mechanical properties, is used in electronic appliances, aerospace, coatings and other fields [19–23]. But EP is extremely flammable under heat, and releases a large amount of dense smoke and harmful volatiles, limiting its large-scale application to a certain extent [24]. Therefore, reducing the fire hazard of EP is of great significance to increase its scope of application.

In this study, ZIF-67 was loaded on graphite phase carbon nitride (g-C_3N_4) by electrostatics action to synthesize ZIF-67/g-C_3N_4 (ZC). Silica as an effective solid acid, can not only catalyze polymerization degradation, but also produce synergistic effects with metal oxides, catalyzing polymer degradation products into carbon [25]. Therefore, tetraethyl orthosilicate was hydrolyzed by the sol-gel method, and SiO_2 was introduced to the ZC surface to produce ZIF-67/g-C_3N_4@SiO_2 (ZCS) nanometer hybrid material. When 3 wt% ZCS was incorporated in to EP, the LOI value was high to 26.2%. pHRR and pSPR increased by 46.8% and 45.2% respectively. In addition, through cone calorimeter, Raman, XRD to discuss the ZCS flame retardant mechanism.

2. Experimental section

2.1. Preparation of g-C_3N_4

G-C_3N_4 was produced by a two-step calcination method in static nitrogen atmosphere. In this procedure, 10 g urea (AR, Aladdin) was poured into crucible and kept at 80 °C for 5 h in a tube furnace firstly. The temperature raised to 540 °C with 20 °C·min^{-1} and maintained for 2 h. When cooled to 25 °C, g-C_3N_4 was obtained after grinding.

2.2. Preparation of ZC hybrid materials

1.5 g g-C_3N_4 was homodispersed in 150 mL anhydrous methanol (AR, Aladdin) and ultrasonicated for 4 h. Then, 150 mL $Co(NO_3)_2{\cdot}6H_2O$ (AR, Aladdin) methanol solution (0.067 M) was added into the above dispersion dropwise. After reacting for 2 h, 150 mL 2-methylimidazole (AR, Aladdin) methanol solution (0.293 M) was also added dropwise for further reaction for 4 h to acquire ZIF-67/g-C_3N_4 (ZC) suspension. Finally, the ZC hybrid material was obtained after washing for three times with methanol solution and dried overnight at 70 °C.

2.3. Preparation of ZCS composite materials

Firstly, 1.5 g ZC was dissolved in 150 mL absolute ethanol. Its pH was adjusted to about 9 with $NH_3{\cdot}H_2O$ (AR, Aladdin) solution, and the ZC solution was then dispersed by ultrasound for 30 min. After that, 4.5 mL tetraethyl orthosilicate (TEOS) (AR, Aladdin) and 15.5 mL anhydrous ethanol solution were added into the ZC dispersion and aged for 14 h. Finally, the ZCS product was obtained after centrifuging three times with ethanol and house-made DI water, and dried at 70 °C for 12 h (The specific experimental process is shown in Scheme 1).

2.4. Preparation of EP composites

The preparation process of the EP4 composite material is presented as an example. First, 3 wt% ZCS was added to a certain amount of EP

Table 1
Formulations of EP and EP composites.

Sample	EP (wt %)	MOCA (wt%)	ZIF-67 (wt %)	g-C_3N_4(wt %)	SiO_2(wt %)	ZC (wt %)	ZCS (wt %)
EP0	77	23	0	0	0	0	0
EP1	74.7	22.3	0	3	0	0	0
EP2	74.7	22.3	0	0	0	3	0
EP3	74.7	22.3	0.9	1.2	0.9	0	0
EP4	74.7	22.3	0	0	0	0	3

(Industrial grade, Shandong Liang New Material Technology Co., Ltd, epoxy value: 0.44) with stirring for 1 min. A fixed amount of melted 4,4-Diamino-3,3′-dichlorodiphenylmethane (MOCA) (Industrial grade, Jinan Shengda Chemical Co., Ltd) was then added into the mixing system and stirred for 1 min. Next, the mixture was poured into a Teflon mold and placed overnight at room temperature, followed by curing at 110 °C and 150 °C for 2 h. After cooling, EP4 composite material was obtained. Other composite materials were produced by the same method (See the specific formulations from Table 1).

2.5. Characterization

The infrared spectroscopy test was performed with a Nicolet model 6700 device (Thermo Fisher Scientific, USA), at wavenumber range of 400–4000 cm^{-1}. X-ray diffraction (XRD) was performed with using a D8X diffractometer (Bruker Company, Germany), with a scanning range from 5° to 70°. Each sample was observed at 20 kV under high vacuum using a Sirion series, model 200 scanning electron microscope (FEI USA). Thermogravimetric analysis (TGA) was performed with a Q5000 series thermal analyzer (TA USA) under an oxygen atmosphere at a heating rate of 20 °C·min^{-1}. The quality of the sample was controlled at about 5 mg and the temperature between 40 °C and 800 °C. The limit oxygen index (LOI) value of the sample was detected by HC-2 (China). The experiment followed the ASTM D2863-2012 standard and the sample size is 100 × 10 × 3 mm^3. The UL-94 vertical combustion of the sample was detected with a px-001 instrument (Suzhou Phoenix Instrument Co., Ltd). The GB/T 2408-2008 standard was applied in the experiment. The sample size is 125 × 13 × 3 mm^3. CONE testing was conducted with an 8610 type cone calorimeter (Suzhou Vouch Company, China) according to the ISO5660–1:2002 standard. The size of each sample was 100 × 100 × 3 mm^3, with aluminum foil backing, at a heat flux of 50 kW/m^2. Carbon residue powder was tested by Spex 1403 laser Raman instrument (USA) at 514.5 nm at about 25 °C.

3. Results and discussion

3.1. Characterization of ZCS

Fig. 1 shows the XRD spectra of ZIF-67, g-C_3N_4, ZC, and ZCS. It can observe that the characteristic peaks corresponding to the (011) (002) and (112) crystal planes of ZIF-67 are located at 7.4°, 10.4° and 12.8°, respectively [26]. And the characteristic peaks at 13.1° and 27.4° are corresponding to the (100) and (002) crystal planes of g-C_3N_4 [27]. For ZC and ZCS, the characteristic peaks related to ZIF-67 and g-C_3N_4 can be found separately. It is worth noting that a peak of ZCS located at 23° is also observed, which is ascribed to the existence of SiO2 in ZCS composites [28].

In Fig. 2, for ZIF-67, due to the in-plane bending vibration of the imidazole ring, a series of sharp characteristic peaks are observable in the range of 900–1350 cm^{-1}. The typical peak at 1350-1500 cm^{-1} is caused by stretching vibration of imidazole ring. The C-N bond and Co-N bond correspond to the characteristic peaks at 1580 cm^{-1} and 424 cm^{-1}, respectively, which are caused by the stretching vibration [29]. For g-C_3N_4, characteristic peak at around 3165 cm^{-1} is caused by stretching vibration of N-H and -OH. The characteristic peak of CN heterocyclic compound in the range of 850–1800 cm^{-1} is attributed to its stretching vibration. The characteristic peak at 811 cm^{-1} is attributed to the typical respiratory vibration of the triazine ring [30]. In addition to the vibration peaks of ZIF-67 and g-C_3N_4, there are also characteristic peaks of SiO_2 in the infrared spectrum of ZCS. The asymmetric tensile vibration peak of Si-O-Si bond and the bending vibration peak of Si-O bond can be observed at 1078 cm^{-1} and 466 cm^{-1}, respectively [31].

Fig. 3 shows the SEM of ZIF-67, g-C_3N_4, ZC and ZCS, respectively. In Fig. 3a, ZIF-67 has a regular diamond-shaped dodecahedron structure, and its size is about 1 μm. In Fig. 3b, g-C_3N_4 is composed of solid agglomerates with a layered structure. In Fig. 3c, it can be clearly seen that ZIF-67 and g-C_3N_4 are uniformly mixed together to form ZIF-67/g-C_3N_4

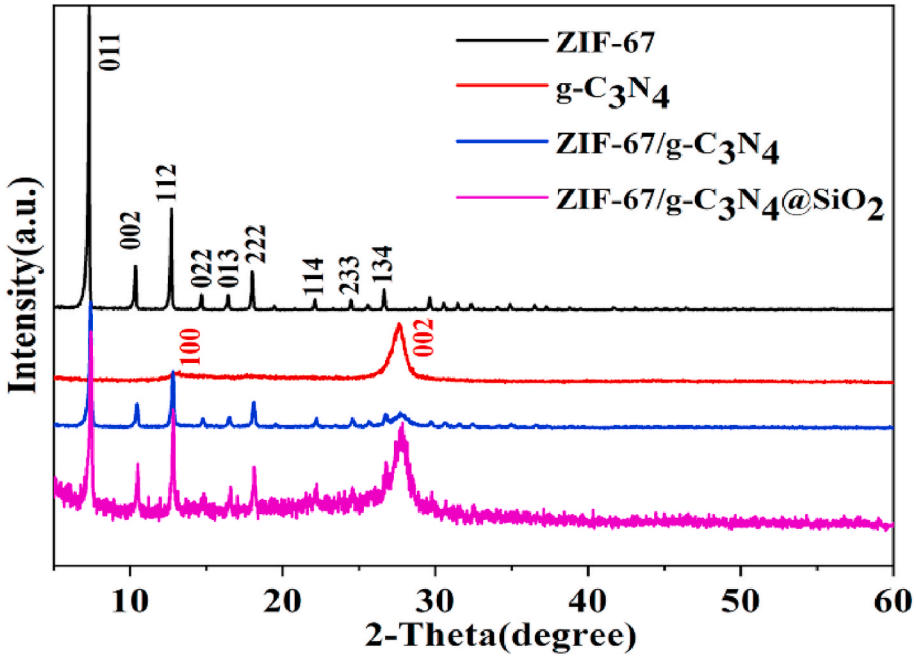

Fig. 1. XRD patterns of ZIF-67, g-C_3N_4, ZC and ZCS.

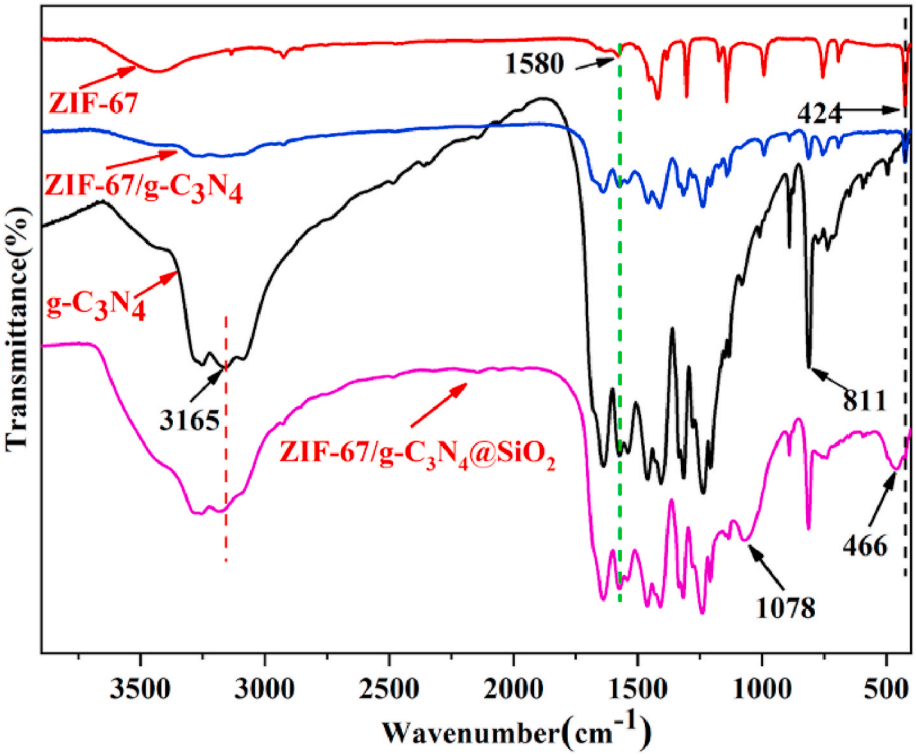

Fig. 2. FTIR spectra of ZIF-67, g-C_3N_4, ZC and ZCS.

hybrid material, with relatively smooth surface. After being coated with silica, the surface of ZIF-67/g-C_3N_4 hybrid material becomes rough, as shown in Fig. 3d. Fig. 3e and f are EDS of ZC and ZCS, respectively. Compared with ZC, ZCS contains not only elements in ZC but also elements Si and O, which indicates that ZCS may contain SiO_2. Combined with the previous XRD and FTIR analysis, they show that successful preparation of ZCS hybrid material.

Fig. 4 shows the thermogravimetric curves of ZIF-67, g-C_3N_4, SiO_2, ZC and ZCS under air atmosphere. There were three stages of weightlessness in the degradation process of ZIF-67. Firstly, the degradation before 100 °C was attributed to the evaporation of methanol on the surface of ZIF-67. Secondly, the carbonization of the 2-methylimidazole molecules remaining in the pores of ZIF-67 caused the degradation between 100 °C and 345 °C. Finally, the degradation starting from 345 °C was caused by the decomposition of organic groups and the fracture of ZIF-67 skeleton. As for g-C_3N_4, the thermal degradation process had only one stage, which mainly occurred between 570 °C and 760 °C. It also showed that g-C_3N_4 was able to withstand higher temperature. For SiO_2, its degradation was split into three phases. The first phase of weightlessness occurred before 110 °C, which was caused by the physically adsorbed water and solvent. Secondly, the weightlessness occurred between 110 °C and 220 °C, corresponding to the condensation polymerization of the structure of silica network. The last stage of weightlessness occurred between 220 °C and 360 °C, caused by the condensation and dehydration of Silanol groups [32]. But for ZCS, the weightlessness rate was 35.2%, and studies showed that ZIF-67 and SiO_2 improved the thermal stability of g-C_3N_4.

Table .2 shows the TGA char residue of SiO_2, g-C_3N_4, ZIF-67, ZC and ZCS. The char residue can be used to estimate the contents of g-C_3N_4 and ZIF-67 in ZC according to formulas (1) and (2) below. W (ZIF-67) and W (g-C_3N_4) represent their mass percentages in ZC, respectively. M (ZIF-67), M (g-C_3N_4) and M (ZC) represent the TGA char residue of ZIF-67, g-C_3N_4 and ZC, respectively. Therefore, it can be estimated that the ZIF-67 and g-C_3N_4 mass percentage ratio in ZC is about 4: 6. In the ZCS system, using the same method to estimate the mass percentage ratio of ZIF-67, g-C_3N_4 and SiO_2 is about 3:4:3. The flame retardant of EP3 in Table 1 is selected by this ratio.

$$W_{(g-C_3N_4)} = \frac{M_{(ZIF-67)} - M_{(ZC)}}{M_{(ZIF-67)} - M_{(g-C_3N_4)}} \times 100\% \quad (1)$$

$$W_{(ZIF-67)} = 1 - W_{(g-C_3N_4)} \quad (2)$$

$$W_{(ZC)} = \frac{M_{(SiO_2)} - M_{(ZCS)}}{M_{(SiO_2)} - M_{(ZC)}} \times 100\% \quad (3)$$

$$W_{(SiO_2)} = 1 - W_{(ZC)} \quad (4)$$

3.2. Flammability of prepared composites

Fig. 5 presents the limit oxygen index (LOI) of EP and its composite materials. The LOI value of EP0 was observed to be 21.2%, indicating that EP was extremely flammable in air. When the same amounts of g-C_3N_4, ZC, ZCS were added, the LOI values of EP composites were improved to a certain degree. The LOI values of EP1, EP2, EP3, and EP4 were 21.7%, 24.8%, 24.4%, and 26.2%, respectively. Compared with EP0, EP4 showed the most significant improvement. In addition, the UL94 vertical combustion tests were performed on EP and its composites. The results showed that the combustion time of EP0 was long after ignition, and the flame spreads to the fixture, with no rating. The combustion times of EP1, EP2 and EP3 were reduced to varying degrees, but they were still no rating. Fig. 6 shows the combustion situations of EP0 and EP4 at different moments. It can be seen that EP4 went out 24 s after ignition, and 3 s after the second ignition, reaching the V-1 rating. It shows that ZCS had good flame retardancy.

As shown in Fig. 7, a cone calorimeter can be used to further detect the characteristics of EP and its composite materials during combustion [33,34]. Fig. 7(a–c) are the curves of the total heat release rate (THR), heat release rate (HRR), and char yield of EP and its composites, and Table 3 lists the important parameters. It can be seen that the peak heat release rate (pHRR) and THR of EP0 are 1251 kW m^{-2} and 99.1 MJ m^{-2}, respectively. After the addition of different flame retardants, both the

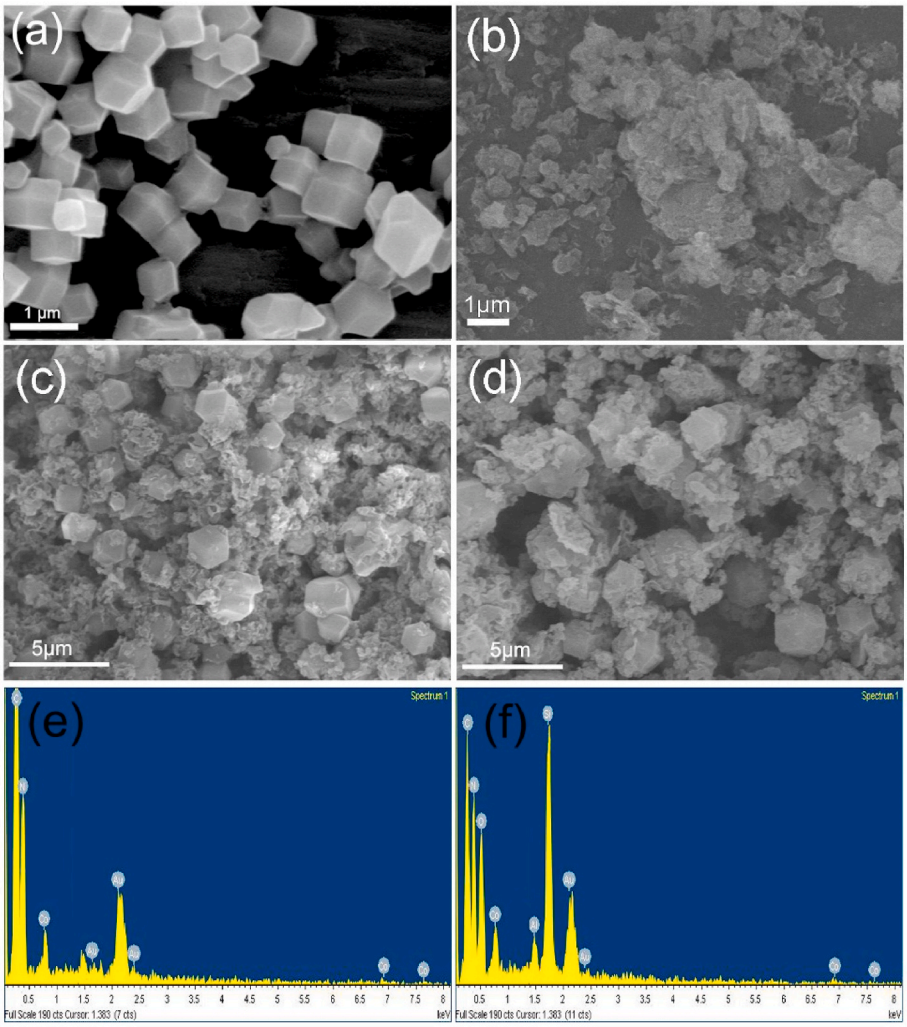

Fig. 3. SEM images of (a) ZIF-67, (b) g-C_3N_4, (c) ZC and (d) ZCS, EDS images of (e) ZC, and (f) ZCS.

pHRR and THR decreased. The pHRR and THR of EP4 were 665 kW m^{-2} and 77.6 MJ m^{-2}, respectively, a reduction by 46.8% and 21.7% compared with those of EP0. Fig. 7c is the curve of the quality loss rate of EP and its composites during the burning process, and Table 3 lists the important parameters. The char residue rate of EP0 at 350 s was 11.4%, while EP1, EP2, EP3 and EP4 had different degrees of improvement compared with EP0. Among them, EP4 had the largest increase of 52.6%. It showed that the addition of ZCS caused the polymer to generate more char residual. It may be ascribed to the -NH_2, -NH and other groups of g-C_3N_4, and the N element contained in ZIF-67, which tend to release NH_3 and N_2 during combustion and attenuation of combustible gas. It is worth noting that, compared with EP0, the av-EHC of EP composites with flame retardants is not significantly reduced. This shows that the role of the hybrid in the gas phase is limited. The lamellar structure of g-C_3N_4 can act as a physical barrier. ZIF-67 will produce metal oxides when burned, thereby catalyzing the formation of carbon layers of polymers. SiO_2 is an effective solid acid that not only catalyzes the degradation of polymers, but also produces a synergistic effect with metal oxides, which can catalyze the degradation products of polymers into carbon. The combination of the three nanomaterials makes the polymer form a denser carbon layer, which blocks oxygen and heat transfer, effectively reducing the fire hazard of the EP composites.

3.3. Smoke suppression of different composites

In addition, smoke and toxic gases are also important indicators to evaluate the safety performance of polymers. Fig. 8 shows the smoke production rate (SPR) and total smoke production (TSP), and CO produced (COP) curves of EP and its composites. Table 3 lists the important parameters. EP released a great amount of smoke during the combustion, and its pSPR and TSP were 0.42 m^2 s^{-1} and 31.1 m^2, respectively. EP1, EP2, EP3 and EP4 with different flame retardants had declined. The pSPR and TSP of EP4 decreased by 45.2% and 19.3%, compared with those of EP0. This may be due to the fact that ZIF-67 produced metal oxides during the heating process, and the large specific surface area adsorbed flue gas particles and volatile particles. As a typical solid acid, SiO_2 can catalyze the degradation of the polymer and migrate to the polymer surface to cover it, delay the burning of the polymer, and reduce the amount of smoke released [28]. In addition, Fig. 8c shows the CO produced curves of EP and its composites. Among them, the pCOP of EP0 is 0.0576 g s^{-1}, and the pCOP of EP4 with flame retardant is 0.031 g s^{-1}, which is 46.2% lower than that of EP0. Adding ZCS effectively reduced the toxic gas in EP and improved its safety performance.

3.4. Char residue analysis of different composites

Fig. 9 shows the SEM images and photographs of residual carbon of EP0, EP1 and EP4. The digital photos show the severely damaged surface of EP0 char residue with large holes. Compared to EP0, the carbon residue surface of EP1 was relatively higher, while its pore size became smaller. The char residue surface of EP4 was denser and the amount of char residue was increased. It was evident that there were lots of holes

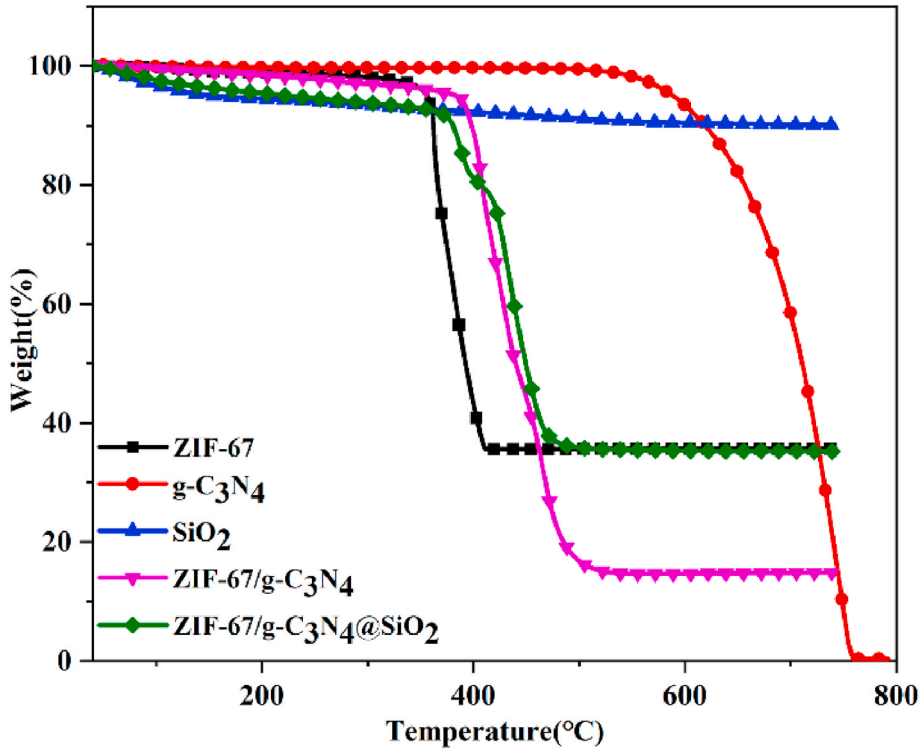

Fig. 4. TGA curves of ZIF-67, g-C_3N_4, SiO_2, ZC and ZCS.

Table 2
Char yield of ZIF-67, g-C_3N_4, SiO_2, ZC and ZCS.

Sample	ZIF-67	g-C_3N_4	SiO_2	ZC	ZCS
Char yield (%)	35.7	0.4	90.2	14.8	35.2

on the char surface of EP0 after combustion, and the carbon residue surface was loose. Compared with EP0, the holes of EP1 were reduced and the carbon residue surface was compact. The char surface of EP4 had almost no holes, and the char residue on the surface was compact and smooth. The carbon layer reduced the transfer of volatile gases and heat, and prevented the polymer from further combustion. The possible reasons are these: first of all, g-C_3N_4 has a physical barrier effect. Secondly, the metal oxides produced by ZIF-67 thermal decomposition can

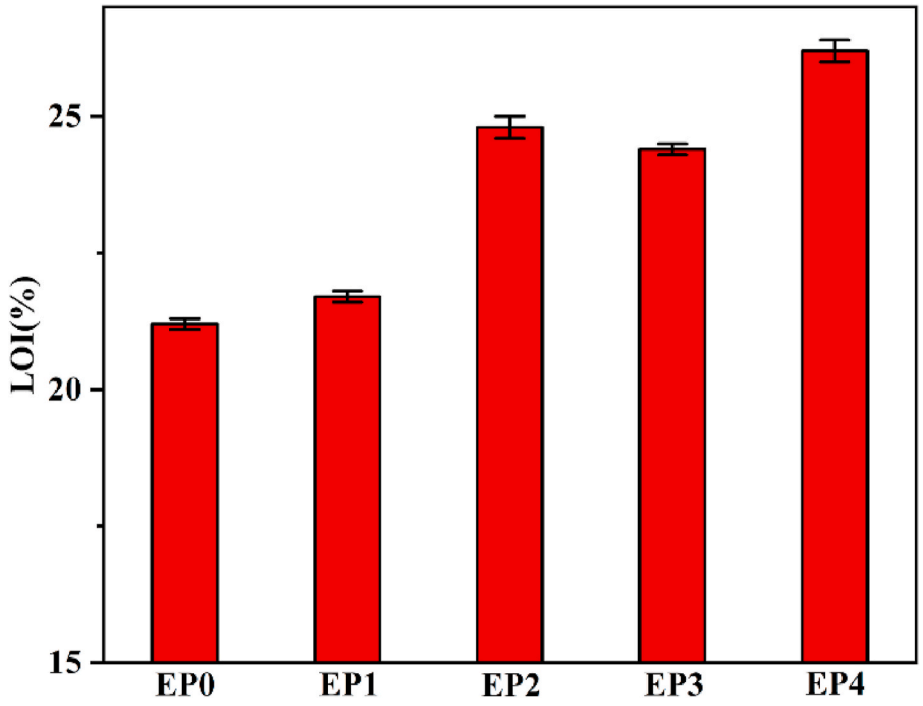

Fig. 5. LOI values of EP and EP composites.

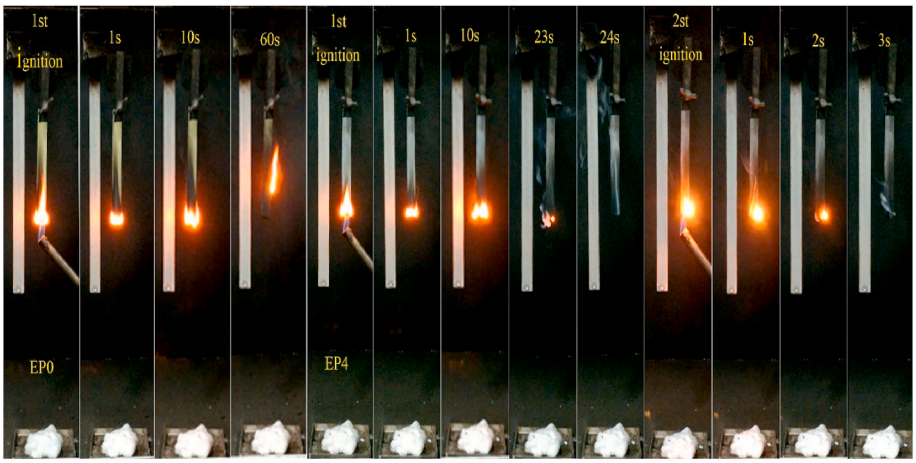

Fig. 6. Combustion processes of EP0 and EP4 during the UL94 vertical burning test at different time.

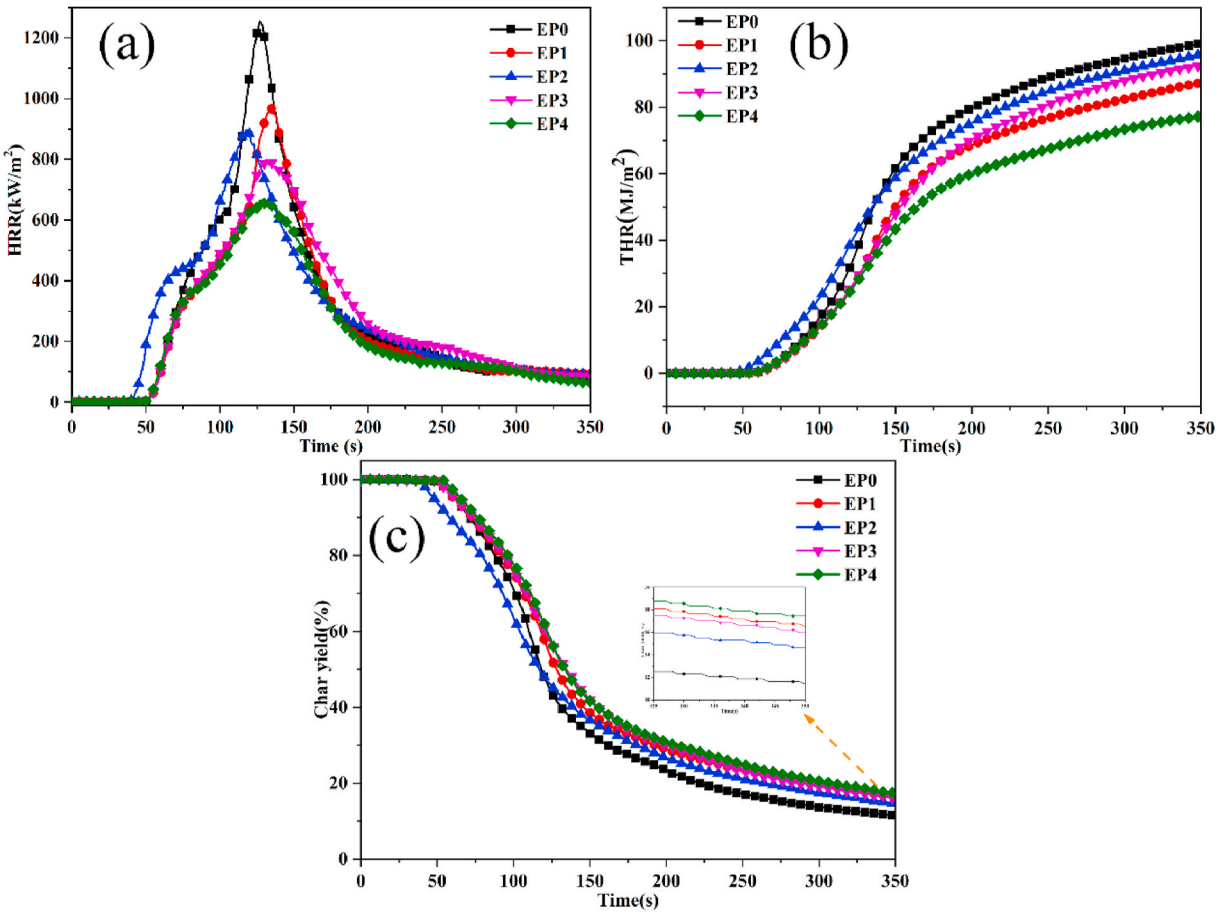

Fig. 7. HRR (a), THR (b) and Char yield (c) curves of EP and EP composites.

Table 3
Date from combustion tests of EP and EP composites.

Sample	pHRR (kW/m^2)	THR (MJ/m^2)	pSPR (m^2/s)	TSP (m^2)	pCOP (10^{-4} g/s)	Av-EHC (MJ/kg)	LOI (%)	UL94 rating	[a]CY_{350} (%)
EP0	1251	99.1	0.42	31.1	576	23.3	21.2	NR	11.4
EP1	966	87.2	0.36	28.7	442	22.6	21.7	NR	16.5
EP2	896	96.0	0.27	27.3	396	22.9	24.8	NR	14.7
EP3	797	92.5	0.27	27.6	340	22.0	24.4	NR	15.9
EP4	665	77.6	0.23	25.1	310	21.3	26.2	V-1	17.4

[a] CY_{350}: the char yield at 350 s.

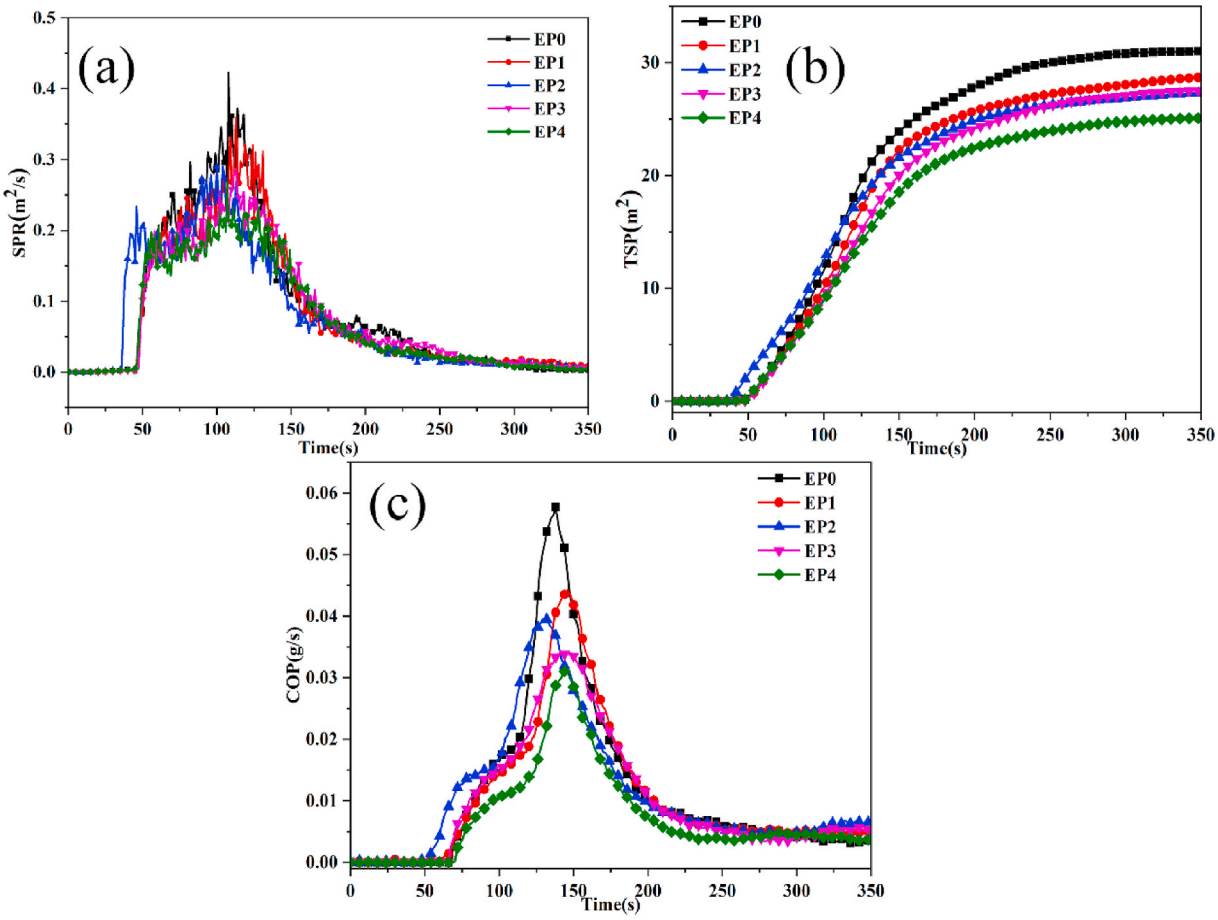

Fig. 8. SPR(a), TSP (b) and COP (c) curves of EP and EP composites.

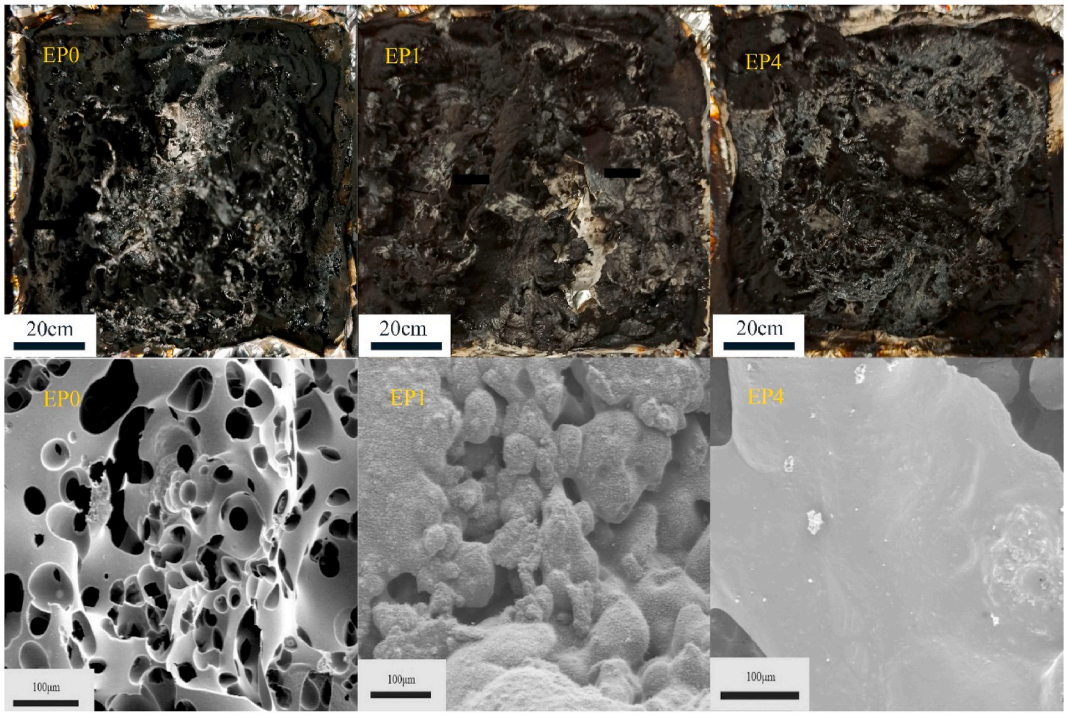

Fig. 9. Digital photos and SEM images of char residue of EP0, EP1 and EP4.

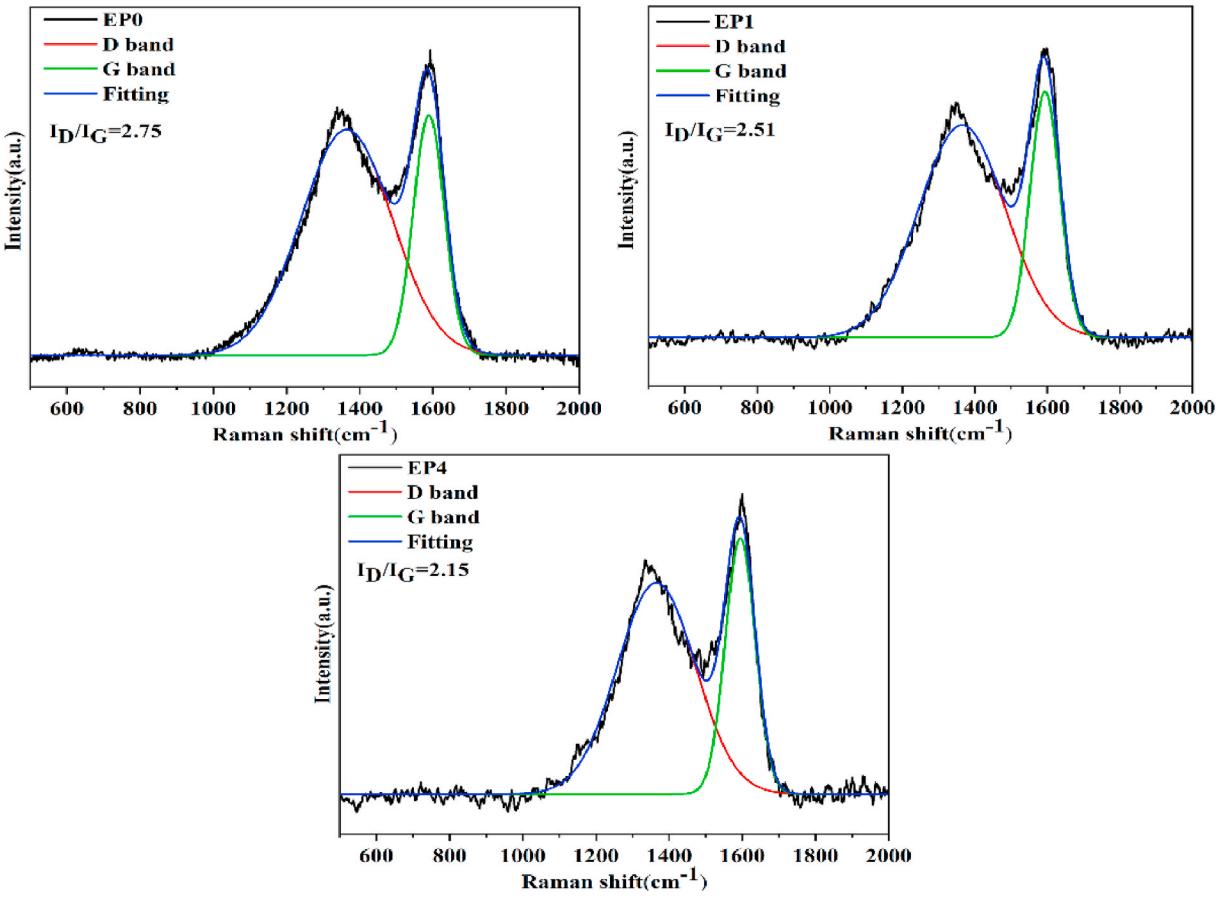

Fig. 10. Raman spectra of char residues of EP0, EP1 and EP4.

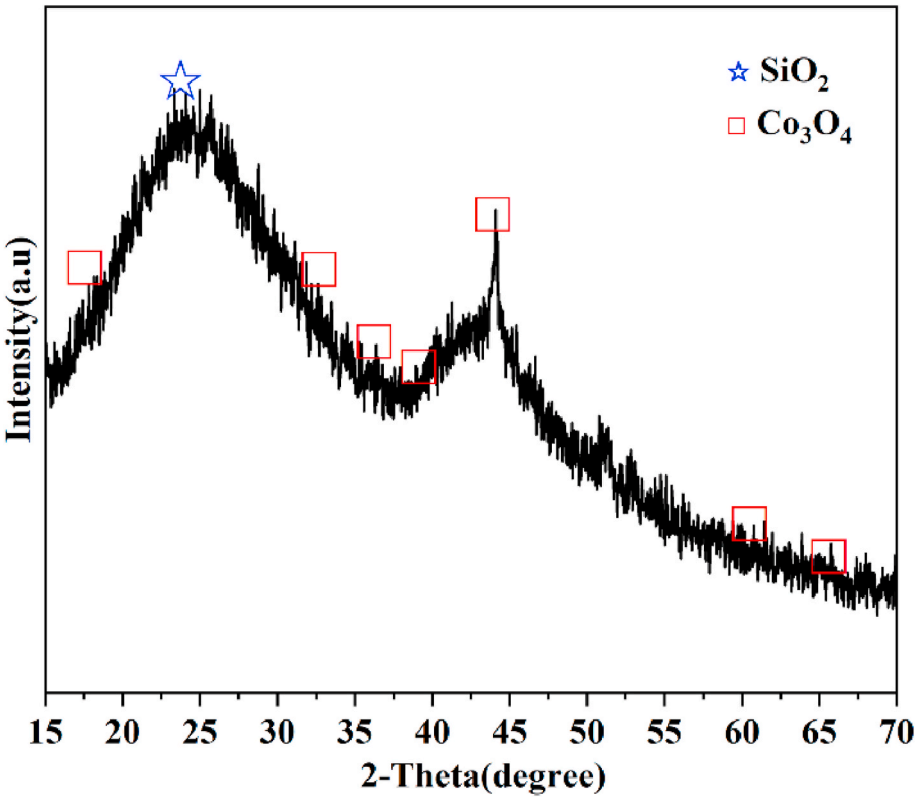

Fig. 11. XRD pattern of char residue of EP4.

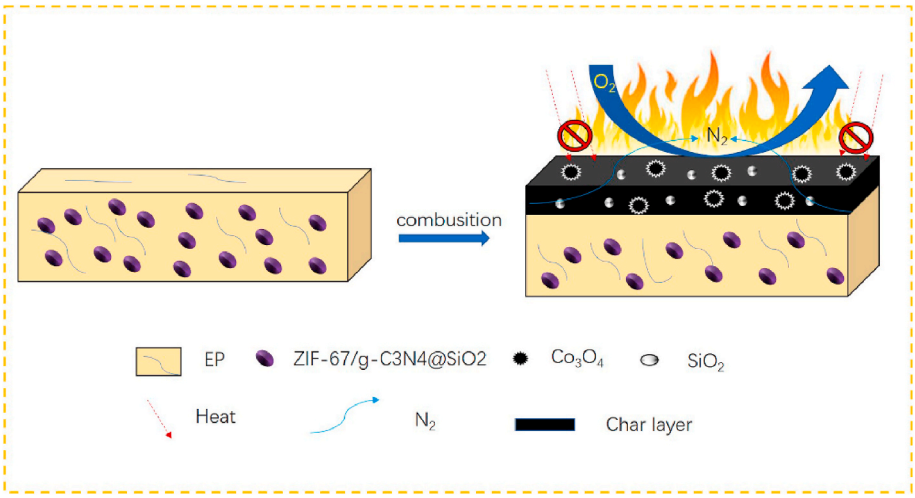

Scheme 2. Illustration for the possible mechanisms of flame retardancy of EP composites.

catalyze the polymer to form a carbon layer. Finally, SiO_2 can be catalyzed in synergy with metal oxides to degrade the polymer into carbon, and effectively shield the direct radiation of the thermal radiation on the substrate, so that the carbon layer and the degree of graphitization are improved. Therefore, adding ZCS led to good char formation performance.

Fig. 10 presents the Ramam spectra of carbon residual of EP0, EP1 and EP4. In Fig. 10, all the char residues have two absorption peaks at 1351 cm^{-1} and 1591 cm^{-1}, which represent the D peak of amorphous carbon and G peak of crystalline graphite carbon, respectively. The ratio of I_D/I_G may help the discussion of the graphitization degree of the residual carbon. Generally, the smaller the I_D/I_G value indicates the higher degree of graphitization [35]. EP4 has the lowest I_D/I_G value of 2.15, which means the highest degree of graphitization. It shows that ZCS can catalyze the formation of carbon layer with high graphitization degree in EP, thereby improving EP flame resistance.

Fig. 11 shows the XRD pattern of carbon residual of EP4. The peak at 23.4° is the characteristic peak of SiO_2 [31]. The peaks at 18.8°, 31.3°, 36.6°, 38.5°, 44.1° and 65.2° are the characteristic peaks of Co_3O_4 [36]. It confirms the existence of SiO_2 and Co_3O_4 in EP4 char residue which catalyze the formation of carbon slag and form a dense carbon layer on the EP surface. Carbon residue reduces the combustible gas and heat transfer to protect the polymer (The possible mechanisms of flame retardancy of EP composites is shown in Scheme 2).

4. Conclusions

In this study, g-C_3N_4, ZIF-67 and SiO_2 were used to synthesize a ZCS composite. The effect of ZCS on reducing the fire risk of EP hidden dangers was studied. The experimental results showed that ZCS had a positive effect on reducing the fire hazard of EP, and its pHRR, THR, pSPR and TSP decreased by 46.8%, 21.7%, 45.2% and 19.3%, respectively. In addition, SEM and Raman results of char residue showed that ZCS can catalyze the polymer to form a highly graphitized carbon layer, reduced the transfer of combustible gases and heat, and consequently prevented the polymer from further combustion. It is hoped that the flame retardant method proposed in this paper will have a positive effect on improving the fire safety of EP materials.

Notes

The authors declare no competing financial interest.

CRediT authorship contribution statement

Wenzong Xu: Writing - review & editing, Conceptualization, Supervision. **Hongyi Yan:** Writing - original draft, Data curation, Methodology. **Guisong Wang:** Software. **Zhongqiong Qin:** Validation. **Liangjie Fan:** Resources. **Yuxiong Yang:** Investigation.

Declaration of competing interest

I declare that we have no known competing financial interests or personal relationships that could have appeared to influence the work reported in this paper.

I declare no financial interest/personal relationship with potential conflict of interest.

Acknowledgements

The authors express their gratitude to the Natural Science Research Project of Colleges and Universities in Anhui Province (KJ2018A0522), Key Research and Development Plan Project in Anhui Province (201904a05020021), Cooperative Innovation Project of Colleges and Universities in Anhui Province (GXXT-2019-001) and Innovative Training Programme for College Students (202010878092) for their support.

References

[1] S. Fazlifard, T. Mohammadi, O. Bakhtiari, Chitosan/ZIF-8 mixed-matrix membranes for pervaporation dehydration of isopropanol, Chem. Eng. Technol. 40 (2017) 648–655.
[2] Z.Q. Li, C.X. Li, X.L. Ge, J.Y. Ma, Z.W. Zhang, Q. Li, C.X. Wang, L.W. Yin, Reduced graphene oxide wrapped MOFs-derived cobalt-doped porous carbon polyhedrons as sulfur immobilizers as cathodes for high performance lithium sulfur batteries, Nano Energy 23 (2016) 15–26.
[3] H. Zhou, D.P. He, L.S. Amiinu, J.L. Yang, Z. Wang, J. Zhang, Q.R. Liang, S. Yuan, et al., Mesoporous-silica induced doped carbon nanotubes growth from metal-organic frameworks, Nanoscale 10 (2018) 6147–6154.
[4] H.X. Liang, X.L. Jiao, C. Li, D.R. Chen, Flexible self-supported metal–organic framework mats with exceptionally high porosity for enhanced separation and catalysis, J. Mater. Chem. A 6 (2017) 334–341.
[5] S.C. Ma, Y.B. Hou, Y.L. Xiao, F.K. Chu, T.M. Cai, W.Z. Hu, Y. Hu, Metal-organic framework@polyaniline nanoarchitecture for improved fire safety and mechanical performance of epoxy resin, Mater. Chem. Phys. 247 (2020), 122875.
[6] Q. Zhou, L.H. Zhu, X.L. Xia, H.Q. Tang, The water-resistant zeolite imidazolate framework-67 is a viable solid phase sorbent for fluoroquinolones while efficiently excluding macromolecules, Microchim. Acta 183 (2016) 1839–1846.
[7] B. Wang, K.Q. Zhou, S. Jiang, Y. Hu, Z. Gui, The application of transition metal molybdates ($AMoO_4$, A=Co, Ni, Cu) as additives in acrylonitrile-butadiene-styrene with improved flame retardant and smoke suppression properties, Polym, Adv. Technol. 25 (2014) 1419–1425.

[8] K.K. Shen, S. Kochesfahani, F. Jouffret, Zinc borates as multifunctional polymer additives, Polym. Adv. Technol. 19 (2010) 469–474.
[9] W.Z. Xu, X.L. Wang, Y. Wu, W. Li, C.Y. Chen, Functionalized graphene with Co-ZIF adsorbed borate ions as an effective flame retardant and smoke suppression agent for epoxy resin, J. Hazard Mater. 363 (2019) 138–151.
[10] Q.H. Kong, Y. Zhang, X. Zhang, B. Xiang, Y.Z. Yi, J.Y. Zhu, F. Zhang, J. Zhu, J. H. Zhang, Functionalized montmorillonite intercalation iron compounds for improving flame retardancy of epoxy resin nanocomposites, J. Nanosci. Nanotechnol. 19 (2019) 5803–5809.
[11] W.H. Li, Q.Q. Chen, Q. Zhong, One-pot fabrication of mesoporous g-C_3N_4/NiS cocatalyst counter electrodes for quantum-dot-sensitized solar cells, J. Mater. Sci. 55 (2020) 10712–10724.
[12] G. Zhang, P. Wang, W.T. Lu, G.Y. Wang, Y.K. Li, J.J. Gu, X.S. Zheng, F.F. Cao, Co nanoparticles/Co, N, S tri-doped graphene templated from in-situ formed Co, S co-doped g-C_3N_4 as an active bifunctional electrocatalyst for overall water splitting, ACS Appl. Mater. Interfaces 9 (2017) 28566–28576.
[13] X.C. Wang, K. Maeda, A. Thomas, K. Takanabe, G. Xin, J.M. Carlsson, K. Domen, M. Antonietti, A metal-free polymeric photocatalyst for hydrogen production from water under visible light, Nat. Mater. 8 (2009) 76–80.
[14] Z.W. Chen, T.T. Chen, Y. Yu, Q.W. Zhang, Z.Q. Chen, J.C. Zhang, Metal-organic framework MIL-53 (Fe)@C/graphite carbon nitride hybrids with enhanced thermal stability, flame retardancy, and smoke suppression for unsaturated polyester resin, Polym. Adv. Technol. 30 (2019) 2458–2467.
[15] A.W. Wang, C. Lee, H.D. Bian, Z. Li, Y.W. Zhan, J. He, Y. Wang, J. Lu, et al., Synthesis of g-C_3N_4/silica gels for white-light-emitting devices, part. Part, Syst. Charact. 34 (2016), 1600258.
[16] K. Pramoda, U. Gupta, M. Chhetri, A. Bandyopadhyay, S.K. Pati, C.N.R. Rao, Nanocomposites of C_3N_4 with layers of $MoS_2$and nitrogenated RGO, obtained by covalent cross-linking: synthesis, characterization, and HER, activity, ACS Appl. Mater. Interfaces 9 (2017) 10664–10672.
[17] Y.Q. Shi, B. Yu, K.Q. Zhou, R.K.K. Yuen, Z. Gui, Y. Hu, S.H. Jiang, Novel $CuCo_2O_4$/graphitic carbon nitride nanohybrids: highly effective catalysts for reducing CO generation and fire hazards of thermoplastic polyurethane nanocomposites, J. Hazard Mater. 293 (2015) 87–96.
[18] Y.L. Zhu, Y.Q. Shi, Z.Q. Huang, L.J. Duan, Q.L. Tai, Y. Hu, Novel graphite-like carbon nitride/organic aluminum diethylhypophosphites nanohybrid: preparation and enhancement on thermal stability and flame retardancy of polystyrene, Composites Part A 99 (2017) 149–156.
[19] Q.H. Kong, T. Wu, J.H. Zhang, D.Y. Wang, Simultaneously improving flame retardancy and dynamic mechanical properties of epoxy resin nanocomposites through layered copper phenylphosphate, Compos. Sci. Technol. 154 (2018) 136–144.
[20] X.D. He, W.C. Zhang, R.J. Yang, The characterization of DOPO/MMT nanocompound and its effect on flame retardancy of epoxy resin, Composites Part A 98 (2017) 124–135.
[21] D.D. Xie, Y.M. Han, K.Q. Zhou, C.L. Shi, In situ polymerization of aniline on the surface of manganese oxide nanosheets for reducing fire hazards of epoxy, Mater. Chem. Phys. 243 (2020), 1226000.
[22] K.Y. Li, C.F. Kuan, H.C. Kuan, C.H. Chen, M.Y. Shen, J.M. Yang, C.L. Chiang, Preparation and properties of novel epoxy/graphene oxide nanosheets (GON) composites functionalized with flame retardant containing phosphorus and silicon, Mater. Chem. Phys. 146 (2014) 354–362.
[23] S.L. Qiu, X. Wang, B. Yu, X.M. Feng, X.W. Mu, R.K.K. Yue, Y. Hu, Flame-retardant -wrapped polyphosphazene nanotubes: a novel strategy for enhancing the flame retardancy and smoke toxicity suppression of epoxy resins, J. Hazard Mater. 325 (2017) 327–339.
[24] X. Wang, Y. Hu, L. Song, W.Y. Xing, H.D. Lu, P. Lv, G.X. Jie, Flame retardancy and thermal degradation mechanism of epoxy resin composites based on a DOPO substituted organophosphorus oligomer, Polymer 51 (2010) 2435–2445.
[25] S.L. Qiu, W.Y. Xing, X.M. Feng, B. Yu, X.W. Mu, R.K.K. Yuen, Y. Hu, Self-standing cuprous oxide nanoparticles on silica@polyphosphazene nanospheres: 3D nanostructure for enhancing the flame retardancy and toxic effluents elimination of epoxy resins via synergistic catalytic effect, Chem. Eng. J. 309 (2017) 802–814.
[26] X.D. Du, C.C. Wang, J.G. Liu, X.D. Zhao, J. Zhong, Y.X. Li, j. Li, P. Wang, Extensive and selective adsorption of ZIF-67 towards organic dyes: performance and mechanism, J. Colloid Interface Sci. 506 (2017) 437–441.
[27] R.Q. Ye, H.B. Fang, Y.Z. Zheng, N. Li, Y. Wang, X. Tao, Fabrication of $CoTiO_3$/g-C_3N_4 hybrid photocatalysts with enhanced H_2 evolution: Z-scheme photocatalytic mechanism insight, ACS Appl. Mater. Interfaces 8 (2016) 13879–13889.
[28] X.X. Wang, S.S. Wang, W.D. Hu, J. Cai, L.H. Zhang, L.Z. Dong, L.H. Zhao, Y.M. He, Synthesis and photocatalytic activity of SiO_2/g-C_3N_4 composite photocatalyst, Mater. Lett. 115 (2014) 53–56.
[29] A. Khan, M. Ali, A. Ilyas, P. Naik, I.F.J. Vankelecom, M.A. Gilani, M.R. Bilad, A. L. Khan, ZIF-67 filled PDMS mixed matrix membranes for recovery of ethanol via pervaporation, Separ. Purif. Technol. 206 (2018) 50–58.
[30] Z.C. Sun, M.S. Zhu, M. Fujitsuka, A.J. Wang, C. Shi, T. Majima, Phase effect of NixPy hybridized with g-C_3N_4 for photocatalytic hydrogen generation, ACS Appl. Mater. Interfaces 9 (2017) 30583–30590.
[31] W.Z. Xu, G.S. Wang, Y.C. Liu, R. Chen, W. Li, Zeolitic imidazolate framework-8 was coated with silica and investigated as a flame retardant to improve the flame retardancy and smoke suppression of epoxy resin, RSC Adv. 8 (2018) 2575–2585.
[32] S.D. Jiang, Z.M. Bai, G. Tang, L. Song, A.A. Stec, T.R. Hull, Y. Hu, W.Z. Hu, Synthesis of mesoporous silica@Co−Al layered double hydroxide spheres: layer-by-layer method and their effects on the flame retardancy of epoxy resins, ACS Appl. Mater. Interfaces 6 (2014) 14076–14086.
[33] A.R. Horrocks, G. Smart, S. Nazare, B. Kandola, D. Price, Quantification of zinc hydroxystannate and stannate synergies in halogen-containing flame-retardant polymeric formulations, J. Fire Sci. 28 (2009) 217–248.
[34] A. Fina, G. Gamino, Ignition mechanisms in polymers and polymer nanocomposites, Polym. Adv. Technol. 22 (2011) 1147–1155.
[35] X.M. Feng, W.Y. Xing, L. Song, Y. Hu, In situ synthesis of a MoS_2/CoOOH hybrid by a facile wet chemical method and the catalytic oxidation of CO in epoxy resin during decomposition, J. Mater. Chem. A 2 (2014) 13299–13308.
[36] E.H. Zhang, Y. Xie, S.Q. Ci, J.C. Jia, Z.H. Wen, Porous Co_3O_4 hollow nanododecahedra for Nonenzymatic glucose biosensor and biofuel cell, Biosens. Bioelectron. 81 (2016) 46–53.